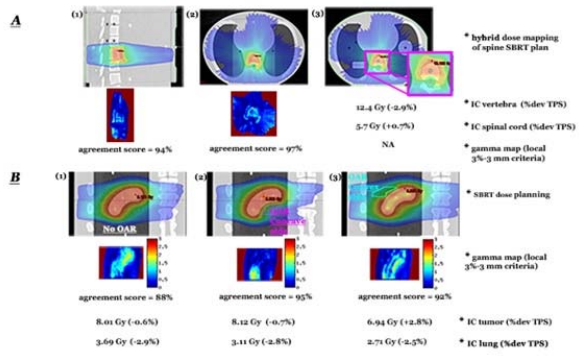

Figure 1: (A) shows the evaluation of spine SBRT with VMAT in (1) the coronal plane of the pelvis part and (2) the axial plane in the thorax part and (3) the plane of IC point of measurement for point dose verification in the vertebrae and spinal canal and (B) shows the coronal dose plan and verification results for the new kidney-shaped tumor volume of E2E CIRS (model 036A) for the situation of (1) no OAR (2) an OAR on the concave side and (3) an OAR on the convex side of the tumor.

Conclusion: A novel, next-generation anthropomorphic phantom allows a versatile SBRT QA, by assessing high dose target coverage and simultaneous OAR dose or peripheral lung dose in an end-to-end testing setup hereby including inter-fraction rotations. The phantom will be the basis of a multi-center peer-to-peer institutional audit of thoracic IMRT/VMAT and SBRT.

EP-1517

Characterization of a new stereotactic diode under flattening filter free beams down to small fields

G. Reggiori[1], P. Mancosu[1], A. Stravato[1], F. Lobefalo[1], L. Paganini[1], F. Zucconi[1], V. Palumbo[1], N. Suchowerska[2], S. Tomatis[1], M. Scorsetti[3]

[1]Humanitas Research Hospital, Medical Physics Service of the Department of Radiation Oncology, Rozzano Milan, Italy

[2]School of Physics- The University of Sydney, Department of Radiation Oncology, Camperdown, Australia

[3]Humanitas Research Hospital, Department of Radiation Oncology, Rozzano Milan, Italy

Purpose or Objective: Stereotactic radiotherapy requires detectors capable of determining the delivered dose with high accuracy. The aim of this study is to characterize the performance of a new unshielded silicon diode prototype, the IBA Razor, for dose measurements in small radiation therapy photon beams in flattening filter free (FFF) mode

Material and Methods: The performance of the newly commercialized stereotactic diode was evaluated relative to that of the previously available SFD diode and the PFD detectors, both from IBA. The Razor is made with an n-type implant in p-type silicon. The active volume is 0.6mm in diameter and 20µm in length. The detector response stability in measured dose, dose rate and dose per pulse were evaluated. Dark current as function of the received dose was also evaluated. The detector response in square fields, in the range from 0.8 to 5.0 cm, was evaluated by means of percentage depth dose curves (PDDs), axial beam profiles and output factors.

Results: The short term stability of the Razor was found to be much improved relative to the SFD, exhibiting a variation of less than ±0.1% for a dose of 1.2 kGy delivered in a single-session. Dose linearity showed a deviation of less than ±1% in the 0.05–30 Gy range and a dose rate dependence of less than ±0.5% in the 4–24 Gy/min range. The dose per pulse dependence, evaluated in the 0.08-0.21 cGy/pulse range, was found to be within ±0.8%. A larger dark current with increase in dose was observed for the Razor with values of 0.0025pA/Gy compared to the 0.0002pA/Gy for the SFD. This characteristic is attributed to an increased concentration of the recombination centers and can be practically solved by resetting the background before every acquisition.
The measured PDDs agreed to within 1% with those obtained using the PFD detector. The profile analysis showed good results as long as a background correction was applied before each profile acquisition: penumbra differences were below ±0.3 mm relative to PFD, with a slight overestimation of the tails (<1%), due to the absence of the shielding. When background correction was not applied regularly, larger differences were observed in the low dose penumbra region and in the profile tails, probably due to the higher dark current. Output factors were in good agreement with those measured by the PFD detector to within 1% for fields up to 5x5 cm^2, for larger fields the absence of the shielding in the stereotactic detector led to differences >2%.

Conclusion: The new IBA Razor unshielded diode replaces the IBA SFD, with the additional advantages of improved stability (up to 1.2 kGy) compared to the reference stereotactic diode. The Razor has the same high spatial resolution and performance in small radiation fields. These features make the Razor diode detector a good candidate for radiation therapy and in small field dosimetry to support advanced radiation therapy techniques.

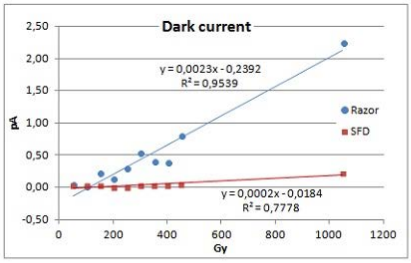

Figure 1 The dark current plotted as a function of the dose to the Razor and the SFD. Diodes.

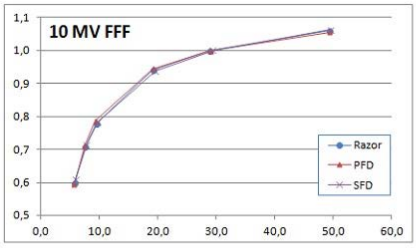

Figure 2 Output Ratios for the three detectors for 10 MV FFF beam. Considered field sizes were 0.6, 0.8, 1, 2, 3 and 5 cm². Volume averaging corrections were applied.

Electronic Poster: Physics track: Dose measurement and dose calculation

EP-1518

Evaluation of dynamic delivery quality assurance process for internal target based RapidArc

J.Y. Song[1], J.U. Jeong[1], M.S. Yoon[1], T.K. Nam[1], S.J. Ahn[1], W.K. Chung[1]

[1]Chonnam National University Medical School, Radiation Oncology, Hwasun, Korea Republic of

Purpose or Objective: In this study, a delivery quality assurance (DQA) method was designed to overcome the limitations of the conventional DQA process in the static condition for internal target volume (ITV)-based VMAT. The dynamic DQA measurement device was designed with a moving phantom that can simulate variable target motions. The dose distribution in the real volume of the target and OARs were reconstructed with the measurement data under the dynamic condition. Then, to evaluate the designed DQA method, the dose-volume histogram (DVH) data of the real target and OARs were compared with the DVHs calculated in the ITV-based VMAT plan.

Material and Methods: The dynamic DQA measurement device was designed with a moving phantom that can simulate variable target motions. The dose distribution in the real volume of the target and organ-at-risk (OAR)s were reconstructed using 3DVH with the ArcCHECK measurement data under the dynamic condition. A total of 10 ITV-based RapidArc plans for liver-cancer patients were analyzed with

the designed dynamic DQA process. Appropriate method was applied to correct the effect of moving phantom structures in the dose calculation, and DVH data of the real volume of target and OARs were created with the recalculated dose by the 3DVH program.

Results: We confirmed the valid dose coverage of a real target volume in the ITV-based RapidArc. The variable difference of the DVH of the OARs showed that dose variation can occur differently according to the location, shape, size and motion range of the target.

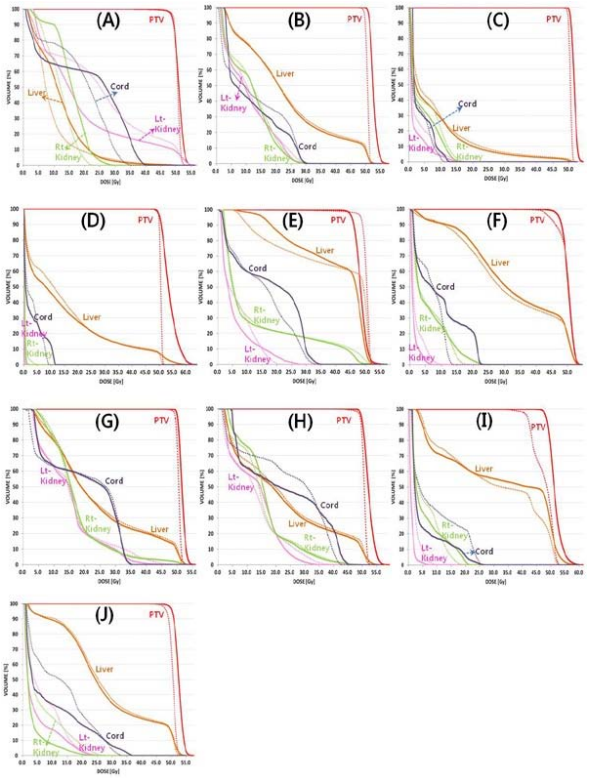

Figure : Total calculated DVH data through dynamic DQA process. Solid line: DVH in the real volume of target and OAR, Dashed line: DVH calculated in the ITV-based RapidArc plan

Conclusion: The conventional DQA method in a static status for the ITV-based RapidArc, without a gating system, can only verify the mechanical and dosimetric accuracy of the treatment machine. An additional DQA method should be devised for evaluating the dosimetric characteristics in the real volume of the target and OARs under respiratory organ motion. The dynamic dose measurement using the moving phantom, which can simulate respiratory organ motions, and techniques employing the measured data to calculate the dose delivered to patients were devised in this study, and proper dose analysis was possible in the real volume of the target and OARs under the moving condition. The devised DQA process appears to be helpful for evaluating the real dosimetric effect of the target and OARs in the ITV-based RapidArc treatment.

EP-1519

Automatic detection of MLC position errors using an EPID based picket fence test

D. Christophides[1], A. Davies[2], M. Fleckney[2]
[1]*St James' Institute of Oncology, Radiotherapy Physics, Leeds, United Kingdom*
[2]*Kent Oncology Center, Radiotherapy Physics, Maidstone, United Kingdom*

Purpose or Objective: The correct calibration of multi-leaf collimator (MLC) leaves is essential in the accurate delivery of radiotherapy treatments, particularly IMRT. In this study EPID picket fence test images are analysed to investigate the possibility to automatically detect intentional errors greater or equal to 0.5mm from baseline MLC errors.

Material and Methods: Picket fence tests were delivered as part of weekly Linac QA in RapidArc mode on Varian iX and 2100CD Linacs equipped with the aS1000 and aS500 EPID respectively. In each QA session a picket fence test was delivered with intentional errors of 0.5mm and 1.0mm; additionally a baseline test was delivered without any intentional errors. A total of 96 picket fence tests were retrospectively analysed covering a period of 6 months.
Using Python v2.7.10 for Windows, an algorithm was implemented to quantify the errors in the MLC positions. Briefly the steps of the algorithm were: 1) Image range calibration, 2) Collimator rotation correction, 3) Isocentre position determination, 4) Derivation of relative leaf positions, 5) Calculation of MLC error from median value at each picket fence field position, and 6) Addition of the errors of opposing leaves at each field position to calculate the combined error (CEr) for each leaf-pair.
The mean and median were calculated from the CEr values of each leaf-pair across the different picket fence field positions. The distribution of the mean and median values calculated was compared between baseline and the intentional MLC errors. Furthermore the normal distribution probability density function was fitted onto all of the baseline CEr data. The mean and standard deviation of the fit were obtained. The t-test and Kolmogorov-Smirnov (KS) statistical tests were used to compare each sample of CEr values obtained from each leaf-pair to the corresponding normal baseline distribution of each Linac examined.

Results: For the Varian iX Linac equipped with the aS1000 EPID the distribution of values of the mean CEr for intentional errors varied between 0.43-1.18mm whereas for the baseline the mean CEr values were between 0.00-0.25mm (Fig. 1). This result showed that the mean CEr can be used to automatically detect MLC errors greater or equal to 0.5mm by setting the detection threshold between 0.25mm and 0.43mm.

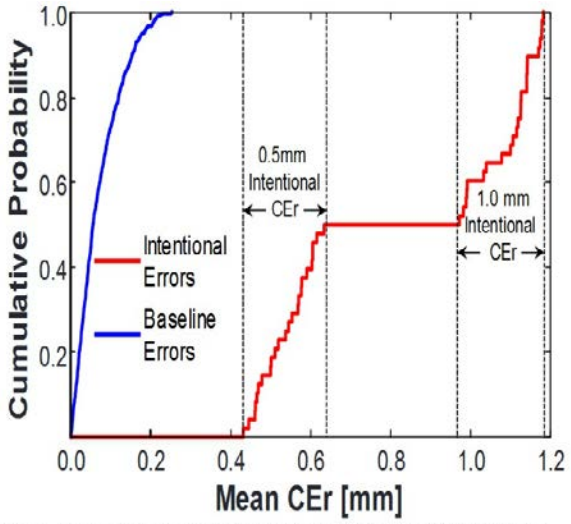

Fig. 1. Cumulative probability distributions of the mean CEr calculated for both baseline and intentional picket fence field errors. Note that there is no overlap in the values between the baseline and intentional mean CEr.

The p-values of the t-tests performed on the data from the Varian 2100CD Linac for the baseline CEr varied between 1.18E-7 and 1.00, whereas for the intentional CEr the p-values were between 0.00 and 5.07E-05. This overlap between the p-values resulted in a false-positive rate of 4.3% if the p-value of 5.07E-5 was to be used as the CEr detection threshold. Table 1 summarizes all the results from the statistical analysis.